Desalination and Water Treatment
www.deswater.com
doi: 10.1080/19443994.2013.808787

51 (2013) 4998–5004
July

Taylor & Francis
Taylor & Francis Group

Experimental evaluation of a modified air-gap membrane distillation prototype

A. Kullab, R. Fakhrai, A. Martin*

Department of Energy Technology/Division of Heat and Power Technology, KTH, Royal Institute of Technology, 100 44 Stockholm, Sweden
Email: andrew.martin@energy.kth.se

Received 31 August 2012; Accepted 2 May 2013

ABSTRACT

Modifications were implemented on a semi-commercial air-gap membrane distillation prototype to assess experimentally any improvement in its performance. The main changes were in the air-gap domain with focus on reducing the conductive heat transfer losses by reducing the physical support that separates the membrane from the condensation surface. Moreover, several feed channel spacers were tested as well and assessed based on their effect in increasing the mass transfer and imposed pressure drop. Results show that the modifications increased slightly the distillate mass flow rate by 9–11% and reduced the conductive heat losses by 20–24%. Spacer effect was found to be mainly in imposed pressure drop within the tested types.

Keywords: Membrane distillation; Conductive heat losses; Experimental work

1. Introduction

Membrane distillation (MD) is a thermally driven process that utilizes a hydrophobic micro-porous membrane to support a vapor–liquid interface. If a temperature difference is maintained across the membrane, a vapor pressure difference occurs. As a result, volatiles (in this case water vapor) evaporate at the hot interface, crosses the membrane in the vapor phase and condenses at the cold side, giving rise to a net transmembrane water flux. The ability of MD to utilize low-grade heat in a form of waste heat/renewable energy source had boosted the interest and research in order to find suitable application areas as well as improving the thermal efficiency of the technology [1].

As the MD is a heat-driven process, several methods has been used to enhance heat transfer coefficient and reduces temperature polarization coefficient. The aspect of heat transfer in all MD configurations is very important and is more believed to be the rate controlling steps in the MD process [2].

Spacers introduced in the flow channel have several roles: keeping the two membrane sheets (constituting the flow channel) apart, achieve better mixing in the direction of the flow and across the flow channel thickness (reduction of the velocity boundary layer

*Corresponding author.

Presented at the Conference on Membranes in Drinking and Industrial Water Production.
Leeuwarden, The Netherlands, 10–12 September 2012.
Organized by the European Desalination Society and Wetsus Centre for Sustainable Water Technology

and thermal boundary layer). On the other hand, they impose an additional pressure drop across the flow channel. The aim of this study is to shed additional light on the role of spacers in a commercial MD module (Scarab Development AB) for the purpose of performance improvements. Detailed computational modeling has been employed in conjunction with the experimental work.

2. Analytical background

2.1. Heat transfer analysis

A typical cross-section of AGMD cassette is shown in Fig. 1. Heat transfer is transferred from the feed solution to the liquid–vapor interface across the thermal boundary layer in the feed channel by convection; then by conduction and latent heat of vaporization across the membrane; then by conduction and latent heat condensation from the permeate side of the membrane to the condensation surface on condensation plate; and finally, by convection from the condensation surface to the cooling liquid across the condensation plate and thermal boundary layer in the cooling channel.

The air-gap domain in AGMD configuration has the role of reducing the conductive heat losses through the membrane surface. In all the theoretical models in AGMD, the assumption is made that the air-gap domain is filled only with air/vapor. However, in practice, the membrane must be supported or separated from the condensation surface by physical means. In trying to avoid the use of support in the lab test, small-scale membrane areas have been considered [3]. One way to support the membrane in plate-and-frame AGMD modules, small ridges or spacer could be used. These ridges can be built-in features of the condensation surface, and hence made from the same material.

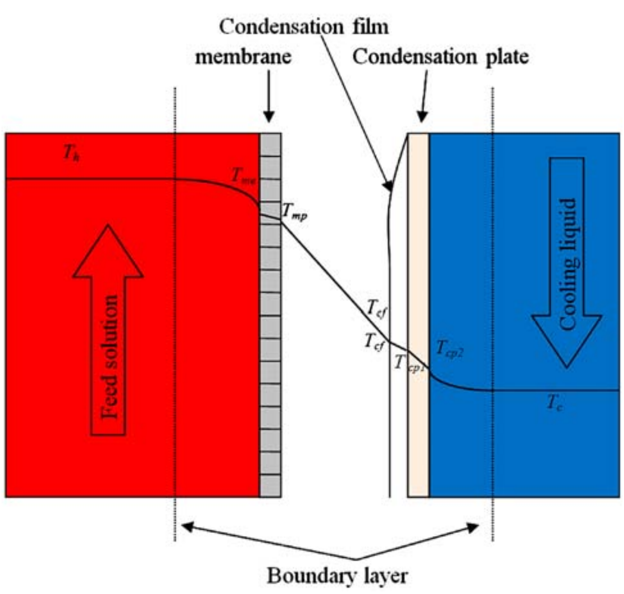

Fig. 1. Cross section AGMD.

These ridges have a negative effect as they reduce the area of membrane and/or condensation surface; they also act as a thermal bridge for conduction. As the thermal conductivity of air/vapor is more than one order of magnitude lower than the thermal conductivity of the ridge (in the case of ridge/condensation surfaces made of polypropylene (PP), covered in this paper); these ridges are the major contributor to the conduction heat losses. In other words, the required cross-sectional area of the air-gap must be 10 times more for the case of equal conduction shares, which is practically impossible even to maintain a reasonable membrane deflection inside the air-gap. The recommended air-gap is usually between 1–3 mm as a trade-off between reducing the conductive heat transfer as a goal, and increasing the mass transfer resistance that the air-gap poses as a penalty. On the other hand, the width of the supporting ridges has a limitation posed by the concern of keeping membrane physical integrity, which in light of the air-gap width and deflection will result in a low area ratio (air to PP ridges). Such ratio hinders the very reason of introducing an air-gap in the first place.

2.2. CFD analysis of obstructed flow channel

Phattaranawik et al. [4] studied experimentally the effect of net-type spacers on heat and mass transfer enhancement in direct contact membrane distillation (DCMD). Experiments were performed on 20 different spacers with different hydrodynamic angles and void ratio. The results showed that spacers enhanced mass fluxes up to 60% and increased heat transfer coefficients by approximately two times over the empty channels. The optimum spacer geometry was found at the void ratio and hydrodynamic angle of 0.6 and 90°, respectively. Martinez et al. [5] performed experiments on two fine and coarse spacers in DCMD configurations. They found that course spacers (void ratio 73%) performed better than fine spacers (void ratio 65%) from transmembrane flux perspective. Despite the positive effect of spacers in increasing the mass fluxes, their performance must be judged in respect to pressure drop they impose, which might have a negative impact on the overall energy efficiency of MD system. Chernyshov et al. [6] studied the effect of five different spacers and on transmembrane flux and pressure drop and compared them to a configuration with an empty channel. They found that the highest flux was achieved by a round filament spacer with hydrodynamic angle of 45˚. However, when comparing the ratio of transmembrane flux with pressure drop, they found that most efficient configuration was the one with empty channel [6]. Computational fluid dynamics (CFD) has been used recently as a method to investigate the effect of spacer on transmembrane flux in reverse osmosis and ultrafiltration.

In case of plate and frame flat sheet MD modules, spacers are not needed to separate the membrane sheets and form the flow channel, though they are still needed as a physical separator to prevent membrane physical contact (for membrane integrity reasons), in addition to their hydrodynamic role. The relative spacer to channel thickness will be one of the area covered in this analysis using CFD as a tool to analyze the hydrodynamic conditions (in particular, flow distribution, pressure drop, and wall/membrane sheer stress) in spacer obstructed flow channel. The physical means by which a spacer that is thinner than the flow channel is kept in the middle of the flow channel will not be discussed in this paper (one way is to attach the spacer element to the frame forming the flow channel). Void ratio and flow of attack angle are two geometrical aspects of spacer that will be covered as well. Fig. 2 illustrates the modeling domain, and Table 1 summarizes the geometrical details of these cases/spacers. All spacers are round-filament nonwoven types with identical diameters of the two filaments constituting the spacer.

Each case was simulated using CD-Adapco CCM + software package. The domain size was chosen large enough to alleviate the entrance region effect. Domain mesh size ranged from 900,000 to 1,500,000 polyhedral finite volume cells depending on the domain size (see Fig. 3 for an example). Mesh was refined and structured close to the membrane surface, and unstructurally refined in the vicinity of the spacer solid and opening parts. When the global mesh number was increased by 10% and near membrane domain mesh by 40%, the difference in results was less than 2%. Convergence criterion for residual of error was set to a minimum of 1×10^{-3} for continuity and the three velocity components. The stability was of the solution was judged by at least 1,000 iterations. Water with constant density was assumed as a fluid. Inlet boundary was chosen as inlet mass flow condition to represent a free stream velocity of 0.011 m/s in all cases, and outlet boundary condition was chosen as pressure (atmospheric). Membrane boundary was chosen to be nonslip condition.

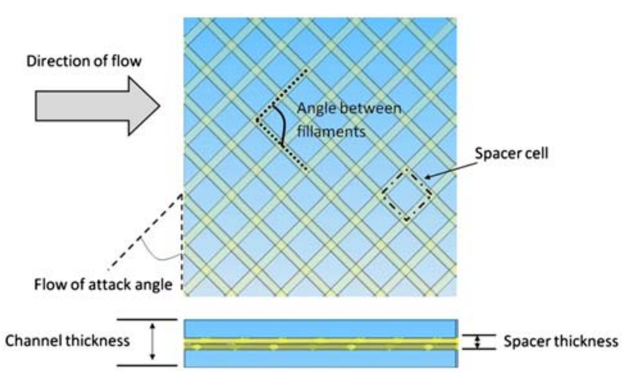

Fig. 2. Schematic of spacer modeling domain.

Table 1
Simulation cases

Case	Flow of attack angle θ (angle between filaments α)	Spacer to channel thickness ratio (TR) %	Void ratio (VR) %
1	37 (105)	23	80
2	52 (75)	23	80
3	45 (90)	23	80
4	45 (90)	46	80
5	45 (90)	69	80
6	45 (90)	100	79
7	45 (90)	46	61
8	45 (90)	46	69
9	45 (90)	46	85
10	45 (90)	46	89

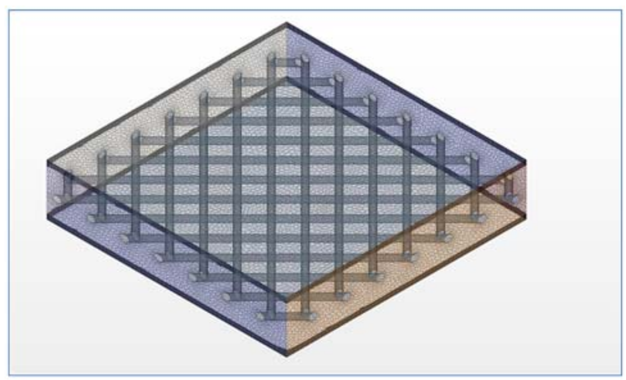
Fig. 3. Example of meshed domain.

Graphical results of the analysis have been presented by Kullab [7] and are omitted here; instead, the ratio of average sheer stress to pressure drop is used to quantitatively assess the spacers. Table 2 lists the average wall (membrane) sheer stress and pressure drop for all cases.

From previous results of cases 1–10, the flow of attack angle (cases 1–3) has a very minimum effect on

Table 2
Average sheer stress and pressure drop

Cases	Average sheer stress (Pa)	Pressure drop per m length (Pa)	Sheer stress/pressure drop ($\times 10^3$)
1 ($\theta = 37^\circ$)	2.77E−02	21.45	1.29
2 ($\theta = 52^\circ$)	2.61E−02	19.2	1.36
3 ($\theta = 45^\circ$) (TR = 23)	2.76E−02	21.11	1.31
4 (TR = 46)	3.02E−02	26.0	1.16
5 (TR = 69)	3.48E−02	35.79	0.97
6 (TR = 100)	2.73E−02	38.49	0.71
7 (VR = 61)	4.820E−02	53.9	0.89
8 (VR = 69)	4.209E−02	43.5	0.97
4 (VR = 80)	3.023E−02	26.0	1.16
9 (VR = 85)	2.524E−02	19.76	1.28
10 (VR = 89)	2.176E−02	15.3	1.42

the performance of spacers. All results of wall shear stress and pressure drop were very close to each other. When it comes to the spacer to channel thickness ratio (cases 3–6), the numerical assessment criteria results suggest the lower ratio is the better; however, one should think that such numerical comparison is very qualitative. In practice, the selection of best case would include a trade-off between the cost of membranes needed to produce the required production and cost of electrical energy needed. (Actually a number of auxiliary equipment – MD modules, piping, fittings, etc. — accompany the cost of membranes.) In all cases, the full channel spacer seems to be the least favorable, at least in case of flat plate MD configurations. When it comes to the void ratio (cases 7–10, 4), the higher void ratio, the better the spacer is. Numerically case 10 would be the favorable spacer. However, such result should be weighed against the membrane cost as the average shear stress, and hence, the heat transfer and specific mass flux would be low.

Some special cases were simulated for different reasons. Case 11 represent two spacers similar to case 3 inserted in the flow channel, in which both can be compared with case 4; i.e. similar spacer to channel thickness ratio and void ratio. This case was simulated because it represents the actual case of MD current design spacer. The other two cases, 12 and 13, have similar characteristic geometries (angle of attack: 45°, spacer to channel thickness ratio: 52%, and void ratio: 87%). The difference is that case 13 has a varying filament diameter with center value of half the value at the crossing node.

Table 3 lists the average wall (membrane) sheer stress and pressure drop for these cases.

Results from cases 12 and 13 are almost similar with flow in the later one having a smoother flow in the vertical and horizontal directions. Comparing cases

Table 3
Average sheer stress and pressure drop (special cases)

Cases	Average sheer stress (Pa)	Pressure drop per m length (Pa)	Sheer stress/ pressure drop ($\times 10^3$)
4	3.02E−02	26.0	1.16
11	4.45E−02	49.6	0.9
12	2.49E−02	19.6	1.27
13	2.27E−02	17	1.33

4 and 11, the numerical indications favorites the case with one spacer since the having two spacers add significantly to the pressure drop without much influence on wall shear stress, as much of kinetic energy is dissipated in the middle region. The numerical efficiency indicator suggests that case 13 is more efficient.

Based on the previous analysis, the main objective of this work is to apply a simple modification on AGMD module in order to improve its performance. These modifications are bounded by the current module design limitations, which include the MD module global dimensions, feed and cooling flow channel thickness and condensation surface material. The main modifications were in the air-gap domain in order to lower the conduction heat transfer transported by the physical support (ridges). Moreover, several spacers similar to the ones simulated in the previous CFD analysis are tested.

3. Modification considerations

3.1. Feed channel

As stated previously, the hydrodynamic conditions significantly affect the heat and mass transfer across the membrane. As spacers are used to affect the hydrodynamic conditions in flow channel in MD, three types of spacers were used to test the effect of spacers' geometry; small cell spacers (two spacers) and large cell spacer. Due to time constraints of this study, the exact geometrical features of the numerically modeled spacers could not be reproduced practically, thus, similar commercially available spacers were chosen for the experimental work (Table 3).

3.2. Distillate/air-gap channel

As mentioned previously, the distillate/air-gap channel consists of small channels formed by several built in ridges. Under working conditions, the membrane sheet is pressed over the ridges and distillate channels are formed. The built-in ridges constitute a thermal bridge for undesirable conductive heat transfer between the membrane and the condensation surface, with approximate area of 25% of the membrane surface. However, only half of these ridges actually serve as conduction medium to the cooling channel, as the other half is connected to the ridges constituting the cooling flow channel/channels (see next section). These ridges were removed and replaced with a nonwoven net-type spacer reducing the area of the conductive medium by 75%. While area of the membrane in contact with spacer (covered by the horizontal filaments) is reduced by 50%, the membrane effective area is still the same as the vertical filaments are in contact with condensing surface. Fig. 4 shows a schematic of the employed spacer. The calculated conductive heat reduction is 30% of original.

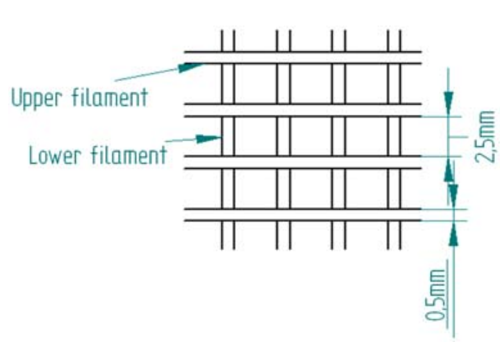

Fig. 4. Schematic illustration of the net type spacer employed as membrane support in the condensation channel.

3.3. Cooling channel

The cooling channel consists of 68 small square flow channels formed by molded PP ridges. These solid ridges reduce the area available for heat transfer by 10%. Moreover, they contribute significantly to higher pressure drop, compared to flow channel with equivalent cross-sectional area due to high wetted perimeter. While these ridges are important to maintain a structural stability for the stacked cassettes, removing these ridges and replacing them with appropriate net type spacer could be a solution to address the hydrodynamic and thermal considerations and in the same time, provide the structural stability.

4. Experimental

4.1. Experimental setup

The test facility (Fig. 5) comprises six-cassette AGMD module with total membrane area of 1.7 m^2 (manufactured by Scarab AB; standard size, 10 cassettes of 2.8 m^2). The cassette consists of injection molded plastic frames containing two parallel membranes, feed and exit channels for the warm water, and two condensing walls. Two sets of condensation/cooling channels plates were used; the original one for establishing a baseline for comparison and the modified one for testing the modified design. The membrane material is PTFE with a porosity of 80%, thickness of 0.2 mm, and average pore size of 0.2 μm. The width of air-gap of AGMD is 1 mm. The size of module is 63 cm wide and 73 cm high. System control and primary data acquisition were handled via PLC connections to Citect Runtime software installed on a standard PC. Flow rates were measured by visual flow meters (accuracy ± 1%), temperatures were measured by Pt 100 s (accuracy 0.2%), and differential pressure with differential pressure transmitters (accuracy 2.5%). On-line conductivity measurements were also introduced to check the instant bulk quality of the product water. Product water flow rate was determined manually. Feed and cooling flow rates were identical for both sides. Tap water of 300–400 μS/cm of conductivity was maintained in the experiments; distillate conductivity was 1–3 μS/cm.

Two sets of experiments were conducted:

- Experiment to evaluate the effect of replacing the solid ridges with spacers in the condensation/air-gap and cooling channel.
- Spacer experiments: aims at choosing the optimum spacer in terms of maximum mass transfer and lower pressure drop (among available spacers).

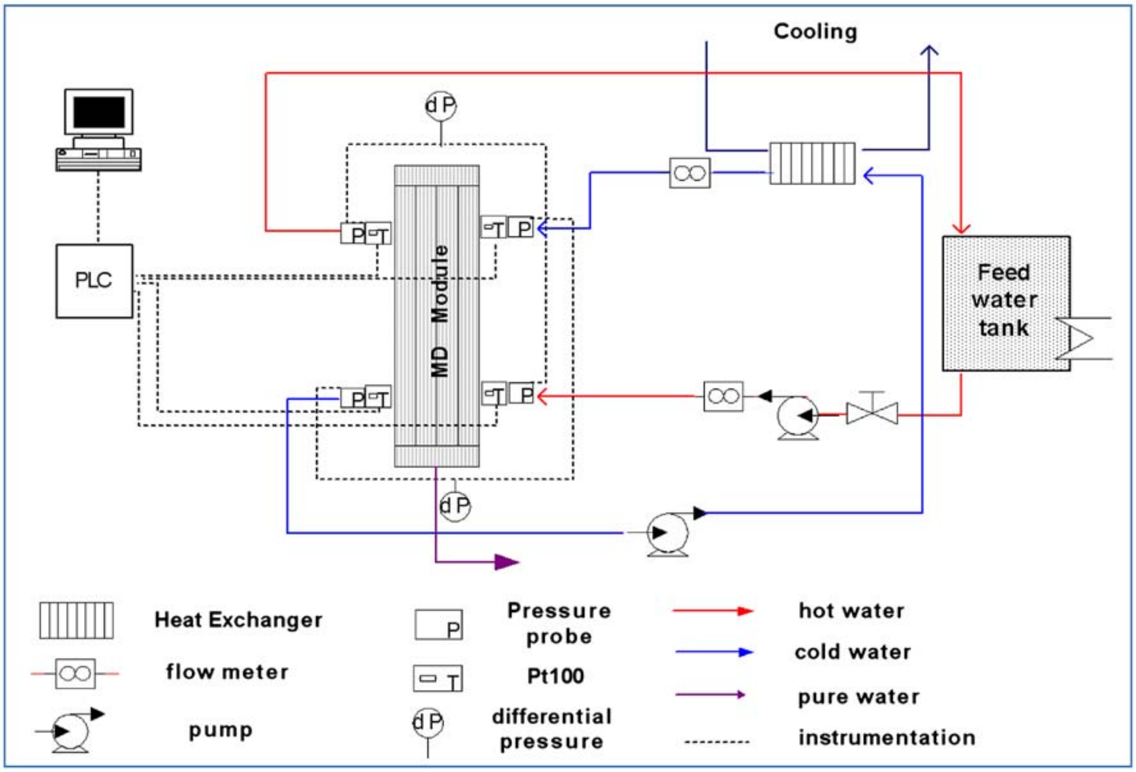

Fig. 5. Schematic illustration of the test rig.

4.2. Experimental results

The experimental results were scaled up for standard MD unit of 10 cassettes.

4.2.1. Original vs. modified condensation/air-gap experiment

Experiments were conducted for both cases at the same operation conditions, feed and cooling flow rates, temperature, and similar type of spacers in the feed/hot channel (spacer 2 in Table 1). Fig. 6 shows the results.

As shown in the figure, the modified configuration is 9–11% higher in distillate flow rate when compared with the original. These results indicate the effect of additional heat available for evaporation caused by lower conduction heat transfer rate.

Fig. 7 shows the thermal efficiency for both original and modified design at varying feed temperatures. The thermal efficiency is defined as:

$$\eta = \frac{Q_L}{Q_T}$$

where QL is latent heat of evaporation and QT is the total heat supplied (including conductive heat).

The thermal efficiency increases with the increase in feed inlet temperature in both cases as known, due to the fact that the rate of increase of latent heat of evaporation is higher, compared to heat transferred by conduction. The thermal efficiency increased by 6% approximately, corresponding to 20–24% reduction compared to the original design.

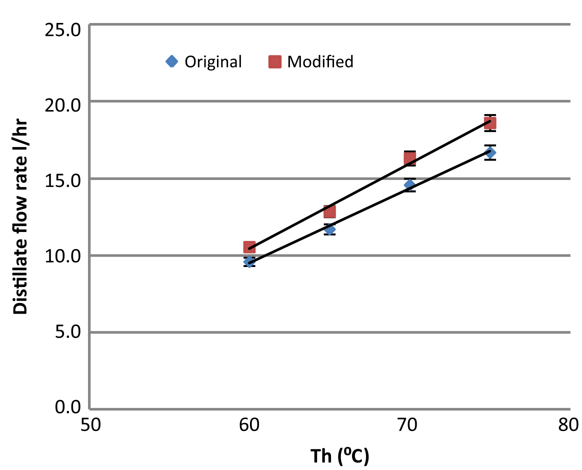

Fig. 6. Experimental results for original vs. modified designs (flow rate of 20 l/min (1,200 l/h), cooling water inlet at 25˚C); error bars depict combined uncertainty.

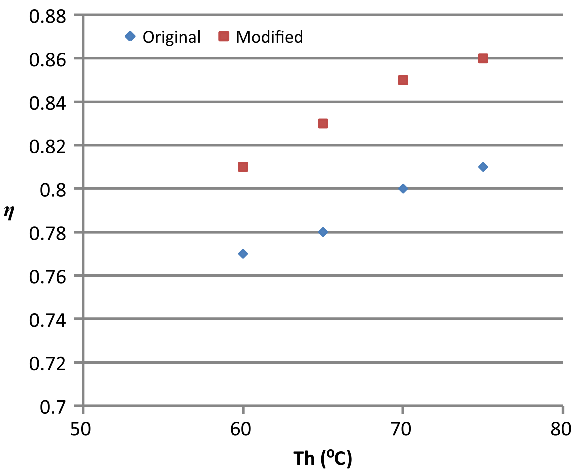

Fig. 7. Thermal efficiency for original vs. modified designs (flow rate of 20 l/min (1,200 l/h), cooling water inlet at 25˚C).

Table 4
Spacer used in experiments

Spacer	Filament diameter (mm)	Cell size (mm)	Flow of attack angle (˚)	Void ratio
1	1.2–2 (varying)	11 × 11	45	86
2	0.75	3 × 3	≈37	80
3	1	3.5 × 3.5	≈35	78

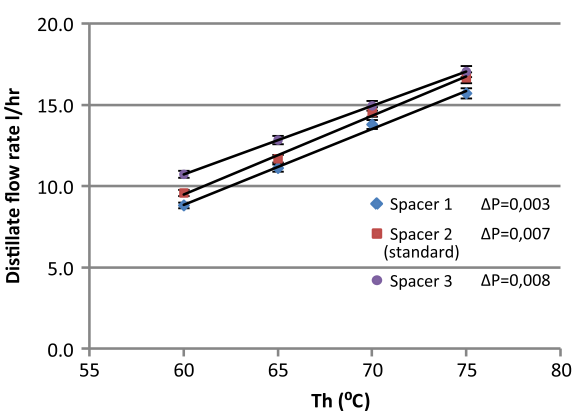

Fig. 8. Experimental results for different spacers (flow rate of 20 l/min (1,200 l/h), cooling water inlet at 25˚C); error bars depict combined uncertainty.

4.2.2. Spacer experiment

Table 4 presents the geometrical details of three different spacers. Spacer 2 represents the original spacer adopted by the manufacturer of the current module.

To use approximately similar spacer to flow channel thickness ratio, one element of spacer 1 (case 13 in CFD simulation) was used, three of spacer 2 (case 11) and 2 of spacer 3. Fig. 8 illustrates the scaled experimental results in terms of distillate flow rate at different feed temperatures.

The results indicate a slightly higher distillate production for the small cell low void ratio spacers compared to the large cell one (spacer 1). As the temperature increases, the distillate flow rate increases for all cases. Nevertheless, the increase is linear which fall short of the theoretical expectation (the exponential trend in MD technology) indicating the high effect of thermal boundary layer at the current used feed flow rate (linear velocity of 0.01 m/s; one order of magnitude lower than most ones reported in literature). Spacers 1 has a significantly lower pressure drop compared to the other two.

5. Conclusion

A possibility of a slight improvement in thermal energy efficiency (6%) with small modifications within the boundaries of geometry and material was demonstrated. Such improvement came as a result of reducing the conductive heat losses, and increasing the area available for heat transfer in general. Since the module was not originally designed with internal heat recovery, a further increase of energy efficiency would be limited.

Acknowledgment

The authors wish to thank both Scarab AB Development and the European Commission (through project Seawater Desalination by Innovative Solar-Powered Membrane Distillation-MEDESOL) for their partial financial support.

References

[1] K.W. Lawson, D.R. Lloyd, Membrane distillation, J. Membr. Sci. 124 (1997) 1–25.
[2] M.S. El-Bourawi, Z. Ding, R. Ma, M. Khayet, A framework for better understanding membrane distillation separation process, J. Membr. Sci. 285 (2006) 4–29.
[3] M. Khayet, T. Matsuura, Membrane Distillation-Principles and application, 1st ed., Elsevier B.V., Oxford, 2011.
[4] J. Phattaranawika, R. Jiraratananon, A.G. Fane, Effects of net-type spacers on heat and mass transfer in direct contact membrane distillation and comparison with ultra studies, J. Membr. Sci. 217 (2003) 193–206.
[5] L. Martinez-Diez, M.I. Vazquez-Gonzalez, F.J. Florido-Diaz, Study of membrane distillation using channel spacers, J. Membr. Sci. 144 (1998) 45–56.
[6] M.N. Chernyshov, G.W. Meindersma, A.B. de Haan, Comparison of spacers for temperature polarization reduction in air gap membrane distillation, Desalination 183 (2005) 363–374.
[7] A. Kullab, Desalination using membrane distillation, PhD dissertation, Department of Energy Technology, KTH, ISSN 1100-7990, 2011.